Preparation and Properties of Optically Transparent Aqueous Dispersions of Monodisperse Fluorinated Colloids

ARTICLE *in* LANGMUIR · OCTOBER 2001

Impact Factor: 4.46 · DOI: 10.1021/la010181y · Source: OAI

5 AUTHORS, INCLUDING:

Gijsje H Koenderink
FOM Institute AMOLF
91 PUBLICATIONS **2,360** CITATIONS

SEE PROFILE

Stefano Sacanna
New York University
48 PUBLICATIONS **1,449** CITATIONS

SEE PROFILE

Albert P Philipse
Utrecht University
189 PUBLICATIONS **6,361** CITATIONS

SEE PROFILE

Preparation and Properties of Optically Transparent Aqueous Dispersions of Monodisperse Fluorinated Colloids

Gijsberta H. Koenderink,* Stefano Sacanna, Chellapah Pathmamanoharan, Mircea Raşa, and Albert P. Philipse

Van't Hoff Laboratory for Physical and Colloid Chemistry, Debye Institute, Utrecht University, Padualaan 8, 3584 CH Utrecht, The Netherlands

Received February 5, 2001. In Final Form: July 19, 2001

We report the emulsion polymerization and seeded growth of negatively charged, monodisperse fluorinated latex spheres in water with radii in the range 50−700 nm. Due to their low refractive index ($n_p = 1.3660$), the spheres can be index matched in aqueous media, without any complications due to (optical) polydispersity or specific solvent adsorption. Such index-matched dispersions of fluorinated latex allow study of the structure and dynamics of strongly interacting charged colloids in water, using light scattering or microscopy. Moreover, we prepared core−shell particles with fluorinated latex shells and optically anisotropic PFA (tetrafluoroethylene copolymerized with perfluoroalkylvinyl ether) cores. We demonstrate with depolarized light scattering that these cores allow for measurement of rotational self-diffusion. The fluorinated latex dispersions are characterized extensively using light scattering, electron microscopy, atomic force microscopy, and electrophoresis. Optical contrast variation is used to determine the particle refractive index and to demonstrate that the particles are optically homogeneous.

1. Introduction

Colloidal dispersions in water are often turbid, which obstructs the use of light scattering techniques to study the structure and dynamics of concentrated colloidal systems. The multiple light scattering in turbid samples can be avoided by using cross-correlation dynamic light scattering[1−4] or by probing samples with neutrons[5] or X-rays.[6,7] An alternative method to avoid multiple scattering is matching the refractive index of the dispersed particles to that of water. Such optical matching has been widely used in organic solvent mixtures, which allow a range of solvent refractive indices sufficient to match, for example, poly(methyl methacrylate)[8] and silica[9] colloids. These colloids, unfortunately, cannot be matched in water with its low refractive index of $n = 1.334$. Water, however, is isorefractive to fluorinated monomers ($n \approx 1.33-1.35$),[10,11] which can be polymerized to latices with a very low turbidity in aqueous suspensions. Examples are PFA (tetrafluoroethylene copolymerized with perfluoroalkylvinyl ether) spheres ($n = 1.362$) which have been used to study rotational diffusion by depolarized light scattering.[12,13] Drawbacks of these PFA latices are the limited size range and the rather complicated synthesis, involving the polymerization of gaseous tetrafluorethylene monomers in an autoclave. Recently, Härtl et al.[14−16] and Pan et al.[17] reported a more convenient synthesis of fluorinated polymer colloids, which can be matched in a predominantly aqueous medium. These promising colloids have been used for instance to prepare colloidal glasses[16] as well as colloidal crystals,[18] which may be suitable for applications such as optical switching devices.[17] In addition, static and dynamic structure factors have been measured by light scattering methods.[14,15,18,19]

Since the fluorinated particles are designed to be model colloids, it is salient that the literature[14,17] does not specify details, or even give a hint, about how to improve control of the sphere size in the polymerization process. Moreover, we found the reported procedure[14] difficult to reproduce. Therefore, we propose a modified synthesis procedure for fluorinated latex colloids. We find that standard synthesis routes for poly(methyl methacrylate), PMMA, polymerization[20,21] can be applied very well to obtain monodisperse fluorinated latices. We also introduce seeded growth as a means to tailor the sphere size. This seeded growth can also be applied to PFA cores, in analogy to the polymerization of polystyrene on PFA seeds.[22] These spherical cores are anisotropic scatterers due to their polycrystalline nature,[12] which makes them very suitable for measure-

* Corresponding author.

(1) Phillies, G. D. J. *J. Chem. Phys.* **1981**, *74*, 260.
(2) Dhont, J. K. G.; de Kruif, C. G. *J. Chem. Phys.* **1983**, *79*, 1658.
(3) Schätzel, K.; Drewel, K.; Ahrens, K. *J. Phys.: Condens. Matter* **1990**, *2*, SA393.
(4) Drewel, K.; Ahrens, K.; Podschus, U. *J. Opt. Soc. Am. A* **1990**, *7*, 206.
(5) Markovic, I.; Ottewil, R. H. *Colloids Surf., A* **1987**, *24*, 69.
(6) Sirota, E. B.; Ou-Yang, H. D.; Sinha, S. K.; Chaikin, P. M.; Axe, J. D.; Fujii, Y. *Phys. Rev. Lett.* **1989**, *62*, 1524.
(7) Riese, D. O.; Vos, W. L.; Wegdam, G. H.; Poelwijk, F.; Grübel, G.; Abernathy, D. *Phys. Rev. E* **2000**, *83*, 1676.
(8) Megen, W. van; Ottewil, R. H.; Owens, S. M.; Pusey, P. N. *J. Chem. Phys.* **1985**, *82*, 508.
(9) Philipse, A. P.; Smits, C.; Vrij, A. *J. Colloid Interface Sci.* **1989**, *129*, 335.
(10) Codding, D. W.; Reid, T. S.; Ahlbrecht, A. H.; Smith, G. H., Jr.; Husted, D. R. *J. Polym. Sci.* **1955**, *15*, 515.
(11) Brandrup, J.; Immergut, E. H. In *Polymer Handbook*; Wiley-Interscience: New York, 1989.
(12) Degiorgio, V.; Piazza, R.; Jones, R. B. *Phys. Rev. E* **1995**, *52*, 2707.
(13) Koenderink, G. H.; Philipse, A. P. *Langmuir* **2000**, *16*, 5631.
(14) Härtl, W.; Zhang-Heider, X. *J. Colloid Interface Sci.* **1997**, *185*, 398.
(15) Härtl, W.; Beck, C.; Hempelmann, R. *Proceedings of the 8th Tohwa University International Symposium*; American Institute of Physics: College Park, MD, 1999.
(16) Härtl, W.; Versmold, H.; Zhang-Heider, X. *J. Chem. Phys.* **1995**, *102*, 6613.
(17) Pan, G.; Tse, A. S.; Kesavamoorthy, R.; Asher, S. A. *J. Am. Chem. Soc.* **1998**, *120*, 6518.
(18) Härtl, W.; Versmold, W.; Zhang-Heider, X. *Ber. Bunsen-Ges. Phys. Chem.* **1991**, *95*, 1105.
(19) Härtl, W.; Beck, C.; Hempelmann, R. *Ber. Bunsen-Ges. Phys. Chem.* **1998**, *102*, 1693.
(20) Ono, H.; Saeki, H. *Colloid Polym. Sci.* **1975**, *253*, 744.
(21) Nieuwenhuis, E. A.; Pathmamanoharan, C.; Vrij, A. *Prog. Colloid Polym. Sci.* **1980**, *67*, 85.
(22) Othegraven, J.; Piazza, R.; Bartsch, E. *Macromol. Symp.* **2000**, *151*, 515.

10.1021/la010181y CCC: $20.00
Published on Web 09/08/2001

ments of rotational sphere diffusion.[12,13] The PFA core thus allows measurement of rotational diffusion in concentrated colloidal suspensions in water, which is a valuable extension of earlier translational diffusivity studies.[14]

Since the fluorinated latices are especially interesting because of their optical properties, we performed light scattering contrast variation according to the method introduced by Vrij,[23] to determine the average refractive index and to quantify any optical inhomogeneity of the particles. This method comprises measuring light scattering intensities as a function of the refractive index difference between particle and dispersing medium (the optical contrast), as explained further in section 2. Section 3 is a detailed description of our synthesis method including the seeded growth. Synthesis procedures and particle properties are evaluated in section 4 using a variety of characterization results, which together underpin our conclusion that the seed-grown fluorinated latices form appropriate model dispersions for charged colloids in water.

2. Light Scattering and Contrast Variation

This section recapitulates some equations needed for analysis of optical contrast variation data. Details can be found in refs 9, 23, and 24. We consider only spherical particles in view of all experimental evidence (see section 4) that our fluorinated latex particles are spherical. The intensity $I(K)$ scattered by optically *homogeneous* spheres of radius R and refractive index n_p dispersed at low weight concentration c in a solvent with refractive index n_s is, within the Rayleigh−Gans−Debye (RGD) approximation,[24] proportional to

$$I(K) \propto c n_s^2 (n_p - n_s)^2 P(K) \tag{1}$$

Here, $K = (4\pi n_s/\lambda_0)\sin(\theta/2)$ is the modulus of the wavevector corresponding to a scattering angle θ and a wavelength in vacuo λ_0. The sphere form factor

$$P(K) = 9\left(\frac{\sin(KR) - KR\cos(KR)}{(KR)^3}\right)^2 \tag{2}$$

has minima at $K_m R = 4.4935, 7.7253$, and so forth, which allows determination of the sphere radius R if one can measure $I(K)$ at sufficiently large KR. For large optical contrasts, Mie scattering shifts the intensity minima to lower wavevectors. Mie contributions can be neglected when the RGD criterion applies, that is, when $(4\pi R/\lambda)|n_p - n_s| \ll 1$.[24] For our aqueous dispersions of fluorinated particles, the RDG criterion is violated only for very large particles ($R > 1\ \mu$m) due to the small optical contrast. For small KR, eq 2 can be written according to the Guinier approximation as[24]

$$P(K) = \exp(-K^2 R_g^2/3) \qquad KR \le 1 \tag{3}$$

so a Guinier plot ($\ln[I(K)]$ vs K^2) yields the radius of gyration:

$$R_g^2 = \frac{3}{5}R^2 \tag{4}$$

To describe the scattering by an optically *inhomogeneous* sphere, consider a spherically symmetric refractive index profile $n(r)$. The average refractive index of such a particle is

$$n_p = \frac{3}{4\pi R^3}\int_0^R n(r) 4\pi r^2\, dr \tag{5}$$

where r is the radial distance from the sphere center. The (average) optical contrast is defined as the difference $n_p - n_s$. The fluctuations $\Delta n_p(r)$ around the average contrast satisfy

$$n(r) - n_s = n_p - n_s + \Delta n_p(r) \tag{6}$$

As a measure for the optical homogeneity of a sphere, one uses a higher moment of the distribution of fluctuations:[9,23]

$$E = \frac{3}{4\pi R^3}\int_0^R \Delta n_p(r) 4\pi r^4\, dr \tag{7}$$

Within the Guinier approximation (KR small), we can rewrite eq 1 as

$$\frac{1}{n_s}\left[\frac{I(K)}{c}\right]^{1/2} \propto |n_p - n_s| \exp[-K^2 R_g^2/6] \tag{8}$$

Instead of eq 4, the optical radius of gyration for an inhomogeneous sphere is[23]

$$R_g^2 = R_{g0}^2 + (n_p - n_s)^{-1} E \tag{9}$$

in which R_{g0} is the radius of gyration at infinite contrast. In our experiments, we vary the solvent refractive index n_s and extrapolate the square root of the intensity $I(K)$ to $I(K) \to 0$, which occurs at a solvent refractive index of n_0 ("the match point"), given by

$$n_0 = n_p - \frac{K^2}{6}E + \ldots \tag{10}$$

as was derived in ref 9. Thus, the average refractive index n_p is obtained from the intensity $I(K\to 0)$, while the intensity at finite K contains information about the optical inhomogeneity E. Sign and magnitude of E can be obtained either by measuring the radius of gyration R_g as a function of the contrast (eq 9) or by determining the match point n_0 as a function of K (eq 10). It should be noted that the above discussion is limited to light scattering. For contrast variation results at large K-values beyond the Guinier region, see for example the recent review on small-angle X-ray scattering of polymeric latices in ref 25.

3. Materials and Methods

3.1. Preparation of Fluorinated Latex Spheres. *Chemicals.* 1*H*,1*H*-Heptafluoro-*n*-butyl methacrylate ($CH_2{=}CC(CH_3)$-$OOCH_2(CF_2)_2CF_3$, 97% Lancaster) was distilled under reduced pressure at 30−40 °C in a nitrogen atmosphere. This monomer has a molecular weight of 254.11 g/mol, a refractive index $n^{20} = 1.3317$, and a density $\rho^{20} = 1.409$ g/mL.[10] The purified monomer was stored under nitrogen at 4 °C. The initiator solution was prepared by dissolving 0.231 g of potassium persulfate ($K_2S_2O_8$, 99+%, Acros Organics) and 0.078 g of sodium bisulfite ($NaHSO_3$, Acros Organics) in 100 g of double-distilled water. In some cases, in addition to the ingredients mentioned, also the negatively charged surfactant sodium dodecyl sulfate (SDS, 99%, BDH Laboratory Supplies, critical micelle concentration[26] of ∼8 mM)

(23) Helden, A. K. van; Vrij, A. *J. Colloid Interface Sci.* **1980**, *76*, 418.
(24) Kerker, M. *The Scattering of Light*; Academic Press: New York, 1969.
(25) Dingenouts, N.; Bolze, J.; Pötschke, D.; Ballauf, M. *Adv. Polym. Sci.* **1999**, *144*, 1.
(26) Aniansson, E. A. G. *J. Phys. Chem.* **1976**, *80*, 905.

was used. This surfactant acts as an emulsifier and also provides additional steric and electrostatic stabilization of the colloids by adsorbing onto the particle surface.[21] (Whether SDS indeed adsorbs onto fluorinated latices, however, has not been established yet by systematic adsorption studies.)

Preparation of Latex Spheres. The fluorinated latex was prepared using emulsion polymerization in water, following refs 20 and 21. The polymerization was done both in the absence and in the presence of 0.75 mM SDS. Typically, 100 g of doubly distilled water and (optionally) 0.0231 g of SDS were added to a three-necked flask, equipped with a magnetic stirrer, a thermometer, and a reflux condenser provided with an attachment for degassing by repeated alternate evacuation and nitrogen purging. The flask was evacuated and saturated with nitrogen after each addition of chemicals. The flask was heated to 70 ± 1 °C by immersion in a thermostated oil bath. The monomer (between 0.2 and 20 mL) was then introduced and emulsified for 1 h at approximately 1200 rpm, using a magnetic stirrer. After the emulsification, the stirring speed was decreased to ∼300 rpm and 5 mL of initiator was added to the reaction mixture. Polymerization was allowed to proceed for 14 h. After typically 15 min, a slightly bluish color was visible, and after another 15 min the turbidity of the mixture visibly increased, manifesting the formation of particles. Some coagulum was usually formed, the amount of which was largest at the largest monomer concentrations and in the absence of soap. The latex suspensions, after filtration to remove coagulum, were either used for subsequent seeded growth or else purified by dialysis against flowing deionized water for 3 weeks, to remove free monomer and emulsifier and residual electrolyte.

Seeded Growth. Seeded growth was done using the same emulsion polymerization method used to obtain the latex seeds, using an identical initiator concentration but without adding any (additional) surfactant. The seed concentration was always fixed at 0.8 wt %, and ≤0.1 M monomer was added dropwise in each growing step. After addition of monomer, we waited at least 14 h before starting the next growing step.

We repeated the same growth experiment using instead of latex spherical Hyflon PFA seeds with a (hydrodynamic) radius of 96 nm, which were a kind gift of Ausimont S.p.A. (Milano, Italy). A detailed description of the properties of such particles can be found in refs 12, 27, and 28. The particles have a crystallinity of 30%, refractive index of 1.362, and a negative surface charge due to an adsorbed anionic perfluorinated surfactant and to carboxyl end-groups generated by the decomposition of the initiator.

3.2. Characterization of Fluorinated Latex Spheres.

Particle Imaging. Scanning electron microscopy (SEM) was performed with a Philips XLFEG30 microscope at 10 kV. SEM samples were prepared by dipping grids in dilute dispersions and coating them with a 5 nm Pt/Pd layer to minimize particle damage (shrinkage, collapse, sintering) due to the electron beam. Even with this metal coating, the latex spheres easily deformed and melted in the SEM electron beam. Interestingly, the PFA particles melted less easily than the fluorinated latex spheres.

Atomic force microscopy (AFM) was performed using a Nanoscope IIIa (Digital Instruments) in tapping mode, on samples prepared by drying a droplet of aqueous latex dispersion on a freshly cleaved mica surface (which was wetted by the dispersion). In some cases (see section 4.4), we used poly-L-lysine coated mica substrates to reduce particle clustering during drying. The substrates were prepared by exposing a freshly cleaved mica surface to an aqueous solution of 0.1−0.7 wt % poly-L-lysine hydrobromide (Fluka, 20−30 kDa) for ca. 30 min. The surface was then rinsed with distilled water and dried in air. Afterward, a droplet of colloidal dispersion was applied on the (now nonwetting) surface. After 10−30 min, the droplet was removed and the surface was dried in air. The drying procedure used for preparing AFM samples flattens the particles considerably. Moreover, contacting particles coalesce to aggregates (we never observed contacting particles which did not flow together to some extent). The easy deformation of latex particles upon drying is consistent with our SEM observations that the latex easily melts in an electron beam (in contrast to PFA particles). We also attempted to image particles dried from 1-propanol, in which the latex forms a stable dispersion. This dispersion, however, did not wet the mica surface very well. Due to the particle deformation observed both with SEM and AFM, we conclude that static and dynamic light scattering are more appropriate for measuring particle sizes.

Table 1. Particle Radius R_{SLS} or R_{DLS}, Variance Factor $Q(K=0)$, Mobility μ, Zeta Potential ζ, and Mass Density ρ_p for Fluorinated Latex Spheres Synthesized with 0.75 mM SDS and Different Monomer Concentrations c_{mon}[a]

c_{mon} [mol/L]	R_{SLS} [nm]	R_{DLS} [nm]	$Q(K=0)$	μ [μm cm s^{-1} V^{-1}]	ζ [mV]	ρ_p [g cm^{-3}]
0.03	48^{G}					
0.05	82^{G}	90	0.0037	−5.8	−80.9	1.59
0.06	63^{G}	70	0.0099	−5.0	−72.7	
0.07	86^{G}	92	0.0023	−5.7	−80.1	
0.08	93^{G}	98	0.0068	−5.8	−80.0	1.63
0.10	112^{G}	121	0.0237	−6.1	−84.0	1.63
0.15	143^{G}	149	0.0126	−6.5	−88.6	
0.20	144^{G}	146	−0.002	−6.7	−90.4	
0.25	157^{min}	154	0.008	−6.6	−89.6	1.63
0.50	184^{min}	190	0.0238	−7.0	−93.1	1.63
1.00	234^{min}	258	0.0048	−5.2	−69.5	

[a] R_{SLS} was determined either from a Guinier plot (superscript G) or from the SLS intensity minima (superscript min). Mass densities ρ_p were obtained from dispersion mass densities measured with an Anton-Paar density meter, thermostatted at T = 25.000 °C.

Particle Sizing by Light Scattering. Static light scattering (SLS) measurements were done on dilute dust-free dispersions, using a FICA-50 photometer at a wavelength λ_0 = 546 nm and a temperature of 25.0 °C. The sphere radius R_{SLS} was obtained using a Guinier plot (eq 3) or the locations of the intensity minima (eq 2). Hydrodynamic radii R_{DLS} were obtained from the Stokes−Einstein diffusion coefficients measured with dynamic light scattering (DLS) on very dilute dispersions at 25.0 °C with an argon laser at a wavelength of 514.5 nm (see Table 1). The same setup was used for depolarized dynamic light scattering (DDLS), but then in vertical−horizontal geometry.[13] DLS intensity autocorrelation functions were fitted to the second-order cumulant expression $\ln g_I(K,t) = \beta_1 + \beta_2 t + \beta_3 t^2$ with fitting parameters β_1, β_2, and β_3. The variance factor, or normalized second cumulant, $Q(K) = \beta_3/\beta_2^2$ provides a measure for the width of the distribution of diffusion coefficients. For small size polydispersities $\sigma \ll 1$, $Q(K=0) \approx \sigma^2$ irrespective of the specific form of the particle size distribution.[29]

Refractive Index and Optical Contrast Variation. Since the refractive index of the latices ($n_p \approx 1.37$) is slightly higher than that of water (n_s = 1.334), aqueous dispersions of fluorinated latex spheres can be easily optically matched by adding glycerol (n_s = 1.475),[14,16,18] urea (n_s = 1.484),[12] dimethyl sulfoxide (DMSO, n_s = 1.476),[17] or 2-propanol (n_s = 1.378).[15,19] In this work, we chose DMSO and 2-propanol as matching agents. The particles are stable in the presence of these compounds, as evidenced by SLS, which showed no detectable change in mean particle radius or size polydispersity over a period of at least several weeks.

Particle refractive indices n_p for λ_0 = 546 nm were obtained from the refractive index increment dn/dc measured with a Brice-Phoenix BP-2000-V differential refractometer at 20 °C. (Note that n is the suspension refractive index and c is the particle weight concentration.) Refractive indices were furthermore determined by performing optical contrast variation.[9] To this end, SLS (λ_0 = 546 nm) was performed on dilute samples of latex spheres dispersed at a constant, low concentration in binary solvent mixtures with varying composition. The intensities were corrected for scattering due to solvent. The solvent refractive index was measured using a Jena refractometer.

Electrophoresis. The zeta potential, ζ, of the particles was estimated from electrophoretic measurements (Coulter DELSA 440 SX) on dilute samples, at a pH of 6, a temperature of 25 °C, and an ionic strength of 20 mM NaCl (i.e., a Debye−Hückel

(27) Piazza, R. *Phys. Scr.* **1992**, *T49*, 94.
(28) Degiorgio, V.; Piazza, R.; Bellini, T. *Adv. Colloid Interface Sci.* **1994**, *48*, 61.
(29) Philipse, A. P.; Vrij, A. *J. Chem. Phys.* **1987**, *87*, 5634.

screening length of $\kappa^{-1} = 2$ nm). The electrophoretic mobilities, μ_e, were converted to zeta potentials using the Smoluchowski equation with Henry's correction term:[30]

$$\zeta = \frac{3\eta\mu_e}{2\epsilon_0\epsilon f_1(\kappa R)} \quad (11)$$

with solvent viscosity η (0.89 cP for water), dielectric permittivity ϵ_0, and dielectric constant ϵ (83 for water). The function $f_1(\kappa R)$ was approximated by

$$f_1(\kappa R) = 1.5 - 4.5/(\kappa R) + 37.5/(\kappa R)^2 - 330/(\kappa R)^3 \quad (12)$$

which is valid for the large experimental κR values ($\kappa R > 20$).[30]

4. Results and Discussion

4.1. Latex Synthesis. In preliminary experiments, we prepared fluorinated latex particles following the emulsion polymerization procedure described by Härtl.[14] Unfortunately, under the conditions described in ref 14, we invariably obtained highly polydisperse particles, as concluded from SLS. Therefore, we introduce a modified procedure, based on another emulsion polymerization recipe used previously for the preparation of PMMA.[20,21] As in Härtl's procedure,[14] the key reagents are a dihydroperfluoro acrylate monomer and a persulfate radical initiator. Reaction conditions, however, are different, which turns out to be crucial for decreasing the polydispersity. An essential step is the use of higher monomer concentrations (0.04−1 M instead of 10−70 mM in ref 14), because for monomer concentrations below 0.04 M we obtained polydisperse particles. Moreover, we work at a higher temperature (70 °C instead of 50 °C), in accordance with the PMMA recipe. We found that the final particle size was different at the two different temperatures, though the monodispersity was not affected. Finally, as an initiator we use $S_2O_8^{2-}/HSO_3^-$, leaving out the $(NH_4)_2Fe^{II}(SO_4)_2$ used by Härtl.[14]

Several factors may influence the particle size obtained in an emulsion polymerization,[31] such as the monomer and initiator concentration,[14,20,21] the temperature, the presence of soap,[21] and the type of stirring.[14] In this study, we limited ourselves to a systematic variation of the monomer concentration in the absence and presence of 0.75 mM SDS. With and without emulsifier, the particle radius increased with monomer concentration from 50 to 260 nm, as shown in Figure 1A. This result agrees with results for PMMA by Fitch,[31] who found that the monomer concentration, within certain limits, affects only the size and not the number of particles formed. Furthermore, we find that up to 0.25 M monomer the particles with emulsifier are bigger than those without emulsifier, while at 0.5 and 1 M monomer the particles without emulsifier are bigger. We also note that in different experiments the particle size was reproduced within 4%, independent of the reactor size (50, 100, 250, or 500 mL).

The particle radii shown in Figure 1A were obtained from SLS measurements, some typical examples of which are shown in Figure 1B. For small particles, ln $I(K)$ versus K^2 is a straight line, as expected from eq 3. For larger particles, the SLS plots deviate from this Guinier approximation and exhibit intensity minima, which shift to smaller wave vectors as the particle size increases. The SLS radii (Table 1) obtained either from the Guinier approximation or from the intensity minima are in good agreement with the radii determined by DLS (Table 1),

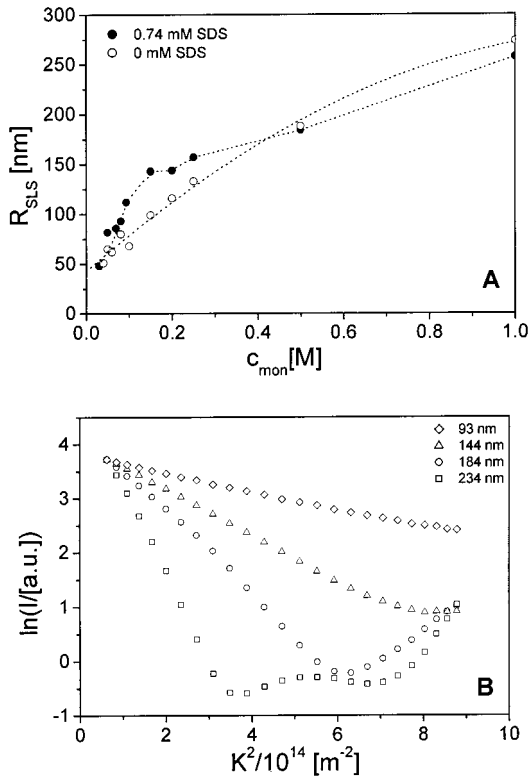

Figure 1. (A) Particle radius versus monomer concentration for fluorinated latex spheres prepared with and without 0.74 mM SDS. (B) Typical Guinier plots, showing the logarithm of the SLS intensity $I(K)$ as a function of K^2, for various latex spheres prepared with 0.74 mM SDS.

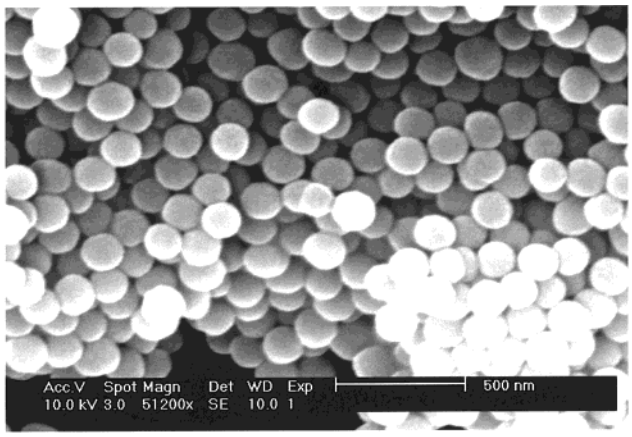

Figure 2. SEM micrograph of fluorinated latex spheres with SLS radius 63 nm, prepared without SDS.

indicating a low size polydispersity, since both techniques measure different moments of the particle size distribution. This low size polydispersity is confirmed by the small values of the normalized second cumulant $Q(K)$ (Table 1), which are usually below 0.01 ($\sigma < 10\%$). Also, both electron microscopy and atomic force microscopy reveal a small size polydispersity (see below).

Figure 2 shows a SEM picture of latex particles with an SLS radius of 63 nm prepared without emulsifier. The particles are spherical to a good approximation, and the size polydispersity is fairly small. Unfortunately, a quantitative determination of particle size and size distribution was obstructed by the particle deformation induced by the electron beam. AFM likewise confirms the narrow size distribution of the latex particles. Figure 3A, for example, shows spheres with an SLS radius of 178 nm

(30) Henry, D. C. *Proc. R. Soc. London, Ser. A* **1931**, *133*, 106.
(31) Fitch, R. M.; Tsai, C. H. *Polymer Colloids*; Plenum Press: New York, 1971.

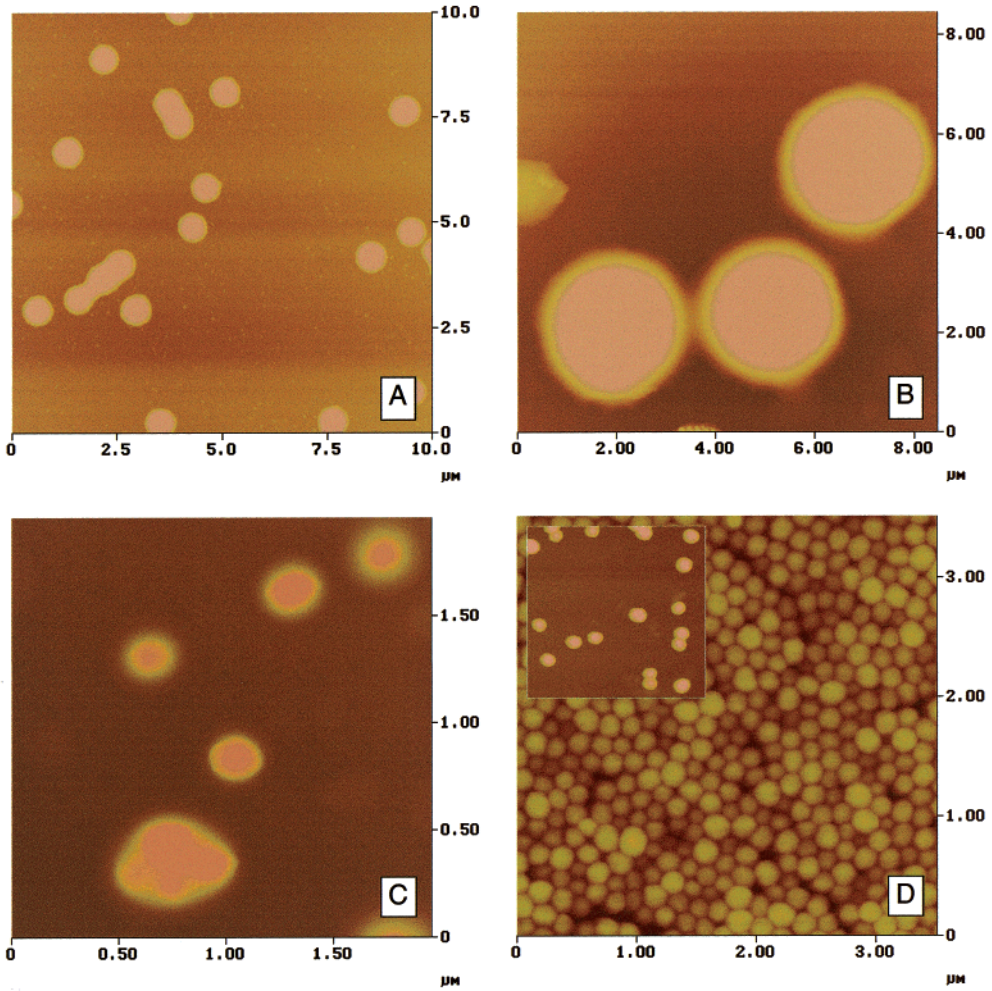

Figure 3. AFM images (tapping mode) of (A) fluorinated latex spheres with SLS radius 178 nm, prepared without SDS; (B) latex core−shell spheres grown in five steps from an SLS radius of 116−735 nm; (C) PFA−latex core−shell particles; (D) a dense monolayer of PFA core particles and single PFA core particles in the inset.

(prepared without emulsifier) with a polydispersity of about 3%. The particles always flatten substantially during the drying procedure. In general, the ratio between diameter and height of the particles is around 10. For instance in Figure 3A, the mean diameter is 717 nm, while the mean height is 88 nm. (For comparison, for silica spheres with an SLS diameter of 130 nm we find with AFM a mean diameter of 141 nm and an average height of 120 nm.) We also observed that contacting latex particles always coalesce to aggregates. The background of the image shows evidence of small precipitates, presumably due to unreacted monomers.

4.2. Contrast Variation. The optical contrast ($n_p - n_s$) was varied by dispersing the particles in mixtures of water/DMSO and water/2-propanol with varying compositions but identical latex concentration. Typical Guinier plots for particles (with a radius of 98 nm prepared without emulsifier) in water/DMSO for several optical contrasts are shown in Figure 4. Striking in Figure 4 is that the shape of the intensity profiles changes little upon approaching the optical match point at about $n_s = 1.37$. Frequently, one finds[9,23] in Guinier plots close to the match point a significant upward curvature at low K. This curvature is attributed to small particle clusters or low levels of contaminants (dust), which become visible in the small-K scattering when the majority of colloids is optically matched.[9,23] Therefore, the data shown in Figure 4 also confirm that the latex spheres have a narrow distribution

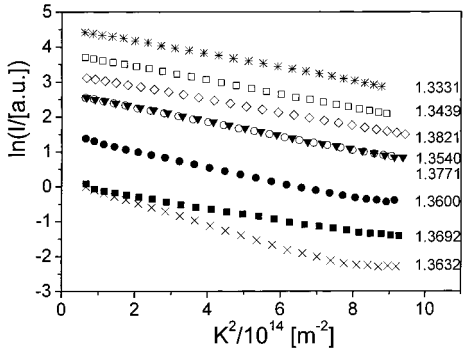

Figure 4. Guinier plots for contrast variation on dilute (0.35 wt %) dispersions of fluorinated latex spheres with SLS radius 98 nm, dispersed in various water/DMSO mixtures ($\lambda_0 = 546$ nm, temperature $T = 25$ °C). Curves are labeled by the refractive index of the solvent mixtures.

of single-particle scattering intensities, with no significant effect of clusters or aggregation.

The match point n_0 as a function of K can be obtained by extrapolating the square root of the intensity $I(K)$ to $I(K) \rightarrow 0$, as shown in Figure 5A for three different K-vectors. The match point n_0, which depends only very weakly on scattering angle (Figure 6A), changes linearly with K^2, in accordance with eq 10. The slope in Figure 6A corresponds to an inhomogeneity parameter of $E = 2.29$ (± 0.09) nm^2. The average refractive index, which is given

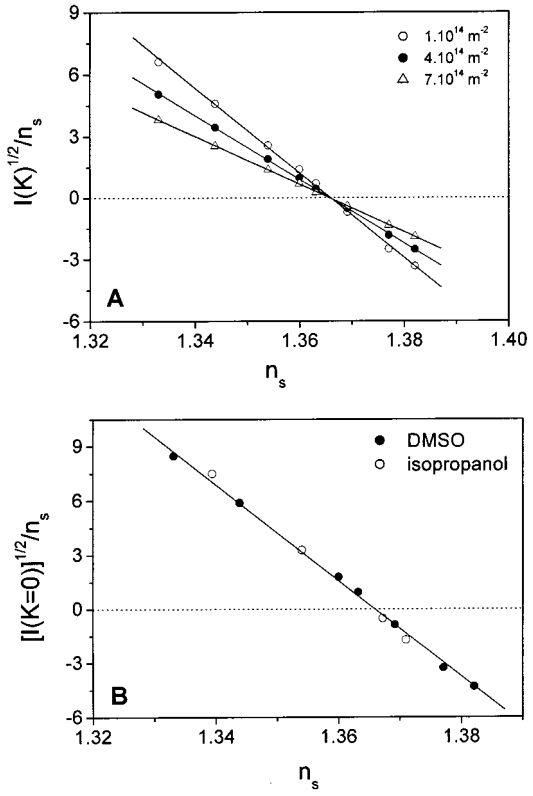

Figure 5. The square root of the intensity (A) $\sqrt{I(K)}/n_s$ for particles in water−DMSO, for three K-vectors as indicated in the legend, and (B) $\sqrt{I(K\rightarrow 0)}/n_s$ for particles in water−DMSO and water−2-propanol versus the refractive index n_s of the solvent mixture.

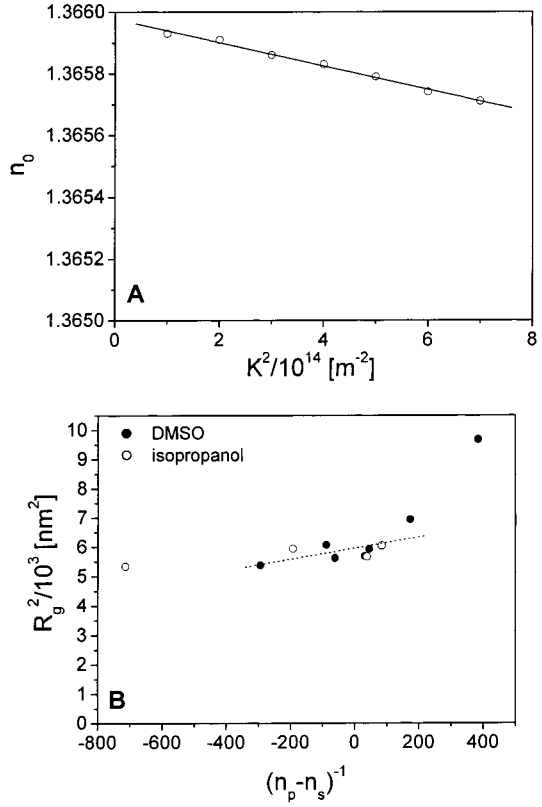

Figure 6. (A) The match point n_0 in a water−DMSO mixture versus K^2. The intercept $n_0(K=0)$ represents the average refractive index, while the slope is proportional to the optical inhomogeneity E. (B) The square of the optical radius of gyration is plotted as a function of the reciprocal contrast. The slope of a linear fit to these data yields the optical inhomogeneity E.

by the intercept $n_0(K=0)$, equals 1.36598 ($\pm 6 \times 10^{-6}$). This compares well to the value $n_0(K=0) = 1.37$ (± 0.02) obtained by the somewhat less accurate procedure of extrapolating the intensities $I(K)$ to $K = 0$ and plotting $\sqrt{I(K=0)}$ versus n_s (Figure 5B). Finally, the result is in line with the refractive index obtained by measuring dn/dc at 20 °C with a Brice refractometer, which yields $n_p = 1.3690$ ($\pm 5 \times 10^{-4}$), using the relation dn/d$c = (n_p - n_s)/\rho$ with the particle density ρ equal to 1.63 g/mL (see Tables 1 and 3). Due to the low refractive index and small optical inhomogeneity of the fluorinated latex spheres, optically transparent dispersions can be obtained by adding a matching agent, such as DMSO or 2-propanol, to an initially turbid dispersion in water (see Figure 7).

The data in Figure 5 agree very well with the linearity $\sqrt{I(K)}/n_s \sim n_s$ predicted by eq 8. This linearity may break down in at least two cases. First, eq 8 assumes identical scatterers; a variation in the (average) refractive index of individual particles will invalidate eq 8. Moreover, for "optically polydisperse" particles the intensity will not become zero at any n_s but will attain a nonzero minimum value. Such a "rest intensity" is not found in Figure 5. The linearity in Figure 5 (and Figure 6) also breaks down when a solvent component preferentially adsorbs onto the particles, as pointed out in ref 23, because then the refractive index profile depends on the solvent composition and, hence, on the contrast. Such adsorption effects, which have been found for silica dispersions,[23] apparently are absent for our latex dispersions.

Additional information about the optical radius and inhomogeneity of the particles also follows from the radius of gyration R_g as a function of the optical contrast. According to eq 9, R_g^2 should depend linearly on $(n_p - n_0)^{-1}$ for sufficiently large contrasts. Figure 6B shows

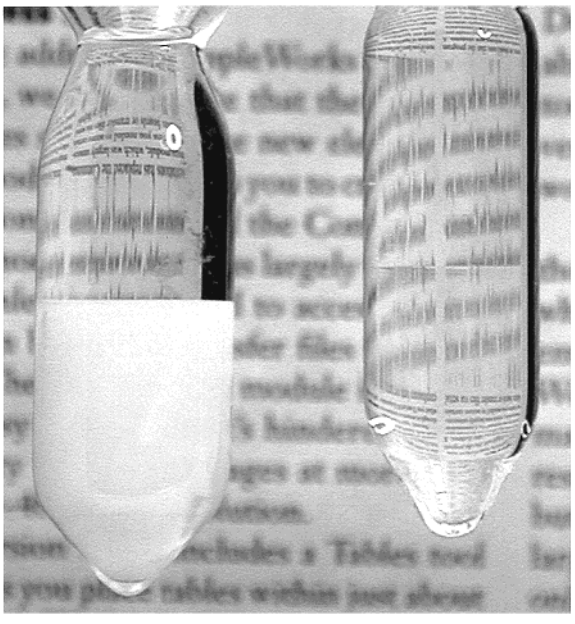

Figure 7. Photographs of (left) a turbid sediment of fluorinated particles with radius 184 nm in water and (right) an optically transparent sediment of the same particles in water/DMSO; note that the transparency is about the same as that of the supernatant.

that R_g^2 is indeed affected by the optical contrast, though the data are rather scattered. The data points for very small contrast are subject to large error and are therefore excluded from the linear fit. Fitting the data in the range $(n_p - n_0)^{-1} = \pm 300$ to eq 9 yields an approximate value

Table 2. Contrast Variation Results

method	$n_0(K=0)$	E [nm^2]	R_{g0} [nm]
n_0 vs K^2	1.36598 ($\pm 6 \times 10^{-6}$)	2.29 ($\pm$0.09)	
$\sqrt{I(K=0)}$ vs n_s	1.37 ($\pm$0.02)		
R_g^2 vs $(n_p - n_s)^{-1}$		1.9 ($\pm$0.8)	77 ($\pm$10)

Table 3. Properties (Same as in Table 1) of Fluorinated Latex Spheres Synthesized without SDS

c_{mon} [mol/L]	R_{SLS} [nm]	R_{DLS} [nm]	$Q(K=0)$	μ [μm cm s^{-1} V^{-1}]	ζ [mV]	ρ_p [g cm^{-3}]
0.04	51^G	57	0.0027	−5.3	−77.9	
0.05	65^G	70	0.0002	−5.4	−77.1	
0.06	62^G	70	0.0003	−5.7	−81.6	
0.08	80^G	84	0.0049	−5.7	−80.6	
0.1	68^G	73	0.0248	−5.5	−78.9	
0.15	99^G	108	0.0093	−6.2	−86.2	
0.2	116^G	125	0.0055	−6.1	−83.7	
0.25	133^G	139	0.0227	−6.0	−81.4	1.62
0.50	178^{min}	199	0.0011	−5.8	−78.2	
1.00	273^{min}	300	0.0029	−5.3	−70.3	

of $E = 1.9$ ($\pm$0.8) nm^2, as well as a radius $R_{SLS} = 100$ ($\pm$14) nm for the equivalent homogeneous sphere at infinite contrast. This value for E is in good agreement with the value $E = 2.29$ ($\pm$0.09) nm^2 determined from $n_0(K^2)$ in Figure 6A. The positive sign indicates a larger refractive index at the periphery than at the center. We will now quantify this particle inhomogeneity by analyzing the parameter E in terms of the refractive index n_R at the periphery of the sphere, that is, at a distance $r = R$ from the sphere center. Suppose n_R is the result of a linear refractive index profile, viz.,

$$n(r) = n_R + \alpha\left(\frac{r}{R} - 1\right) \tag{13}$$

where α is a (positive or negative) constant. From eqs 5 and 7, we can derive for this profile

$$\frac{E}{R_{g0}^2} = \frac{1}{3}(n_R - n_p) \tag{14}$$

which leads to a rather small inhomogeneity of $n_R - n_p = 0.0012$, on substitution of the measured E and R_{g0} from Table 2. For comparison, consider a large homogeneous core with radius γR, supplemented with a thin shell with constant refractive index n_R, to form a sphere with total radius R. For such a core−shell profile, eqs 5 and 7 now lead to

$$\frac{E}{R_{g0}^2} = (1 - \gamma^2)(n_R - n_p) \qquad 0 \le \gamma \le 1 \tag{15}$$

with a second unknown parameter γ in addition to n_R in eq 14. However, for any reasonable value of γ (i.e., the shell thickness) we again find that the optical inhomogeneity is small. For example, a shell thickness of 5% ($\gamma = 0.95$) corresponds to $n_R - n_p = 0.004$. These calculations, of course, do not attempt to provide a realistic refractive index profile $n(r)$; they merely show that refractive index variations in the latex spheres are small, namely, of order 10^{-3} or less. Such small variations are consistent with the very weak dependence (see Figure 6A) of the match point on the wave vector.

4.3. Latex Particle Charge. Electrophoretic mobilities of latices with and without emulsifier are presented in Tables 1 and 3, together with zeta potentials obtained using eqs 11 and 12. The fluorinated latex spheres have negative zeta potentials of typically −70 to −90 mV, both with and without emulsifier. The corresponding negative surface charge is due to the strongly acidic sulfonate ($-SO_3-$) and sulfate ($-OSO_3-$) end-groups generated by the free radical polymerization[14] and, for the SDS-stabilized particles, also to the anionic surfactant. For the particles synthesized with 0.75 mM SDS, the magnitude of the zeta potential increases with particle size, in agreement with results of Härtl.[14] For the particles synthesized without emulsifier, the zeta potential varies between −77 and −86 mV without a clear particle size dependence.

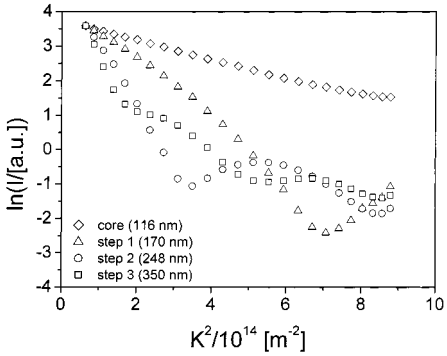

Figure 8. Guinier plots of fluorinated latex core−shell particles obtained by seeded growth of latex cores (radius 116 nm) in the absence of SDS.

Latex dispersions were found to be stable over a wide range of pH and ionic strength. The latex spheres do not aggregate until more than 400 mM NaCl has been added. This remarkably high stability is due to a combination of two factors. First, at low ionic strengths the particles experience strong double-layer repulsions due to their large surface charge. Second, van der Waals attractions will be small due to the small refractive index difference with the solvent. In the case of poly(tetrafluoroethylene) (PTFE), which has a refractive index comparable to that of fluorinated latex, the Hamaker constant in water is only 0.82 kT at room temperature.[32]

4.4. Seeded Growth. The largest particle radius obtained by a single-step emulsion polymerization was 273 nm (see Figure 1). Even larger particles can be prepared by seeded growth. As an example, Figure 8 shows Guinier plots of a series of particles grown in several steps starting from a core with radius 116 nm. As the particles grow, minima develop which subsequently shift to smaller K-vectors. Particles can become as large as 700 nm, as evidenced by Figure 3B, which displays an AFM image of core−shell particles grown in five steps to a total SLS diameter of 1470 nm. Due to the drying procedure used for preparing the sample, the spheres deformed to oblates; they have an apparent diameter of 3000 nm in the AFM image, while their height is only 200 nm (see also section 4.1). Large particles such as those in Figure 3B may be suitable for optical microscopy studies of the structure and dynamics of charge-stabilized particles in water.

We found that fluorinated latex polymerizes not only onto latex cores but also on PFA cores. These PFA particles are optically anisotropic. Therefore, they are suitable for measuring rotational diffusion by DDLS.[12,13] They have a similarly low refractive index as fluorinated latex. Using the same seed (0.8 wt %) and monomer (0.1 M) concentration as for the seeded growth of fluorinated latex, we obtained PFA core−shell spheres with a total DLS radius of 121 nm (120 nm from SLS first minimum). There was

(32) Lyklema, J. *Fundamentals of Interface and Colloid Science*; Academic Press: London, 1993; Vol. 2.

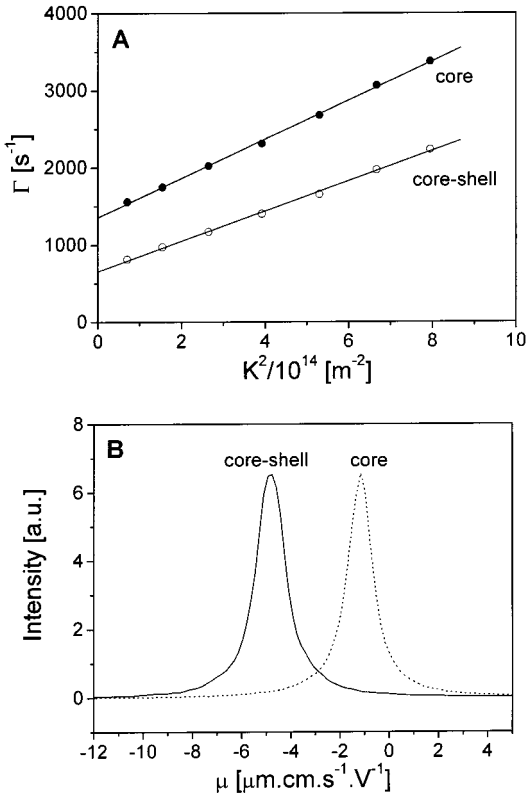

Figure 9. (A) Decay rate Γ of electric field autocorrelation functions measured with depolarized dynamic light scattering at various wavevectors *K*, for PFA core and PFA−latex core−shell particles. (B) Electrophoretic mobility of the same core and core−shell particles (20 mM NaCl).

some secondary nucleation of latex particles with a radius of 61 nm (58 nm from SLS), as seen by DLS. (Secondary nucleation also occurred for 1.6 wt % seeds, 0.05 M monomer, and a slower monomer addition rate.) The two particle species could be easily separated by repeated sedimentation. The resulting supernatant contained only secondary nucleation latex spheres, which are not optically anisotropic (there is no depolarized scattered light signal). The sediment contained only PFA−latex core−shell particles, which give rise to depolarized light scattering. DDLS autocorrelation functions were single-exponential at all scattering angles between 30 and 120°. Figure 9A shows the decay rate Γ of these correlation functions versus K^2 for the PFA cores and for the PFA−latex core−shell particles. In both cases, Γ versus K^2 is linear. The slope of these plots equals the translational diffusion coefficient D^t, while the intercept with the Γ-axis equals 6 times the rotational diffusion coefficient D^r.[13] For the PFA cores, this analysis gave $D^t = 2.53 \times 10^{-12}$ m^2/s ($R = 93.5$ nm) and $D^r = 225$ s^{-1} ($R = 96.9$ nm), while for the core−shell particles $D^t = 1.95 \times 10^{-12}$ m^2/s ($R = 125.6$ nm) and $D^r = 104$ s^{-1} ($R = 121.0$ nm). The radii derived from DDLS are in good agreement with the radii from DLS (97 and 121 nm, respectively). This experiment demonstrates that PFA−latex core−shell particles can be prepared that are suitable for rotational diffusion measurements.

Growing latex onto PFA changes the particle surface potential, as seen from electrophoresis (Figure 9B). The core−shell particles have an electrophoretic mobility of -5.1 μm cm s^{-1} V^{-1}, which is typical for fluorinated latex, while the core particles have a mobility of only -1.2 μm cm s^{-1} V^{-1}; a mobility difference which clearly confirms the latex polymerization onto the PFA cores. When mixed in tracer amounts with concentrated dispersions of fluorinated latex host spheres, one could measure rotational and translational self-diffusion, since tracer and host spheres have the same surface chemistry.

AFM pictures of PFA−latex core−shell particles invariably showed large clusters of PFA particles encapsulated by a latex film. Apparently, the core−shell particles group together during drying, upon which the latex shells merge together while the PFA cores remain intact. The formation of clusters could be largely prevented by coating the mica substrate with the positively charged poly-L-lysine. Figure 3C shows a representative picture of the core−shell particles stuck on poly-L-lysine coated mica. There are several single particles and also one cluster of four particles, which are together encapsulated by a latex shell. The particle (PFA) cores in this cluster have, unlike the latex cores in Figure 3A, not coalesced. This shows that the PFA particles are much less deformable than the latex particles, which is supported by the fact that the diameter/height ratio for the individual particles in Figure 3C is 1.4 instead of 10 (diameter 230 nm, height 160 nm). Each particle seen in Figure 3C is surrounded by a shell with a height of ∼25 nm, which is presumably due to the (deformed) latex shell. The PFA particles before seeded growth do not display this shell (Figure 3D). Figure 3D also confirms that the PFA cores are much more resistant against shape deformation than the fluorinated latex, in line with the SEM observations (section 3.2). The higher resistance of PFA toward deformation is also consistent with its higher density (2.14 g/mL) relative to latex (1.63 g/mL).

5. Conclusions

We have demonstrated that monodisperse fluorinated latex spheres with radii between 50 nm and (at least) 700 nm can be reproducibly prepared, both with and without emulsifier, using emulsion polymerization and seeded growth procedures. Due to their low refractive index (1.3660 at 25 °C) and small refractive index fluctuations (order 10^{-3} or less), these latex spheres can be optically matched in water−DMSO or water−2-propanol mixtures to near complete transparency, without complications due to (optical) polydispersity or specific solvent adsorption. These convenient optical properties, together with a negative surface charge and excellent stability, make the fluorinated particles a promising model system of charged particles to be studied by light scattering, microscopy, or photobleaching. For instance, one might study tracer dynamics in concentrated fluid, glassy, or crystal phases.[18] In this context, our novel core−shell latices with optically anisotropic PFA cores and fluorinated shells are relevant, as such cores allow measurements of rotational sphere diffusion. Conditions for seeded growth (monomer concentration, seed concentration, addition speed, etc.) of latex on PFA will have to be modified to avoid secondary nucleation of latex. The PFA−latex core−shell particles can be used as tracers in combination with latex host particles, to measure rotational and translational self-diffusion in concentrated dispersions of charged spheres.

Acknowledgment. We thank W. Härtl, R. Piazza, and E. Bartsch for helpful discussions. A. Carlone is thanked for doing additional synthesis and characterization work. We are grateful to P. van Mourik (Molecular Biology, Utrecht University), J. E. G. J. Wijnhoven, and G. Bosma for the SEM micrographs. B. W. M. Kuipers is thanked for help with DLS measurements.

LA010181Y